2011 50th IEEE Conference on Decision and Control and
European Control Conference (CDC-ECC)
Orlando, FL, USA, December 12-15, 2011

Binary signals design to control a power converter

Jérémy Van Gorp, Michael Defoort, Mohamed Djemaï

Abstract— **The power converters are more and more implanted to optimize the energetic properties of electrical systems. This paper concerns the control of commutations for a multicellular converter through a hybrid approach. Compared with a classical converter (H-bridge), the structure of the multicellular converter enables a more accurate regulation. In this kind of converter, a complete regulation of the state is required to ensure the tracking of the load current and a suitable distribution of the capacitor voltages across each cell. Using the hybrid formalism, the dynamics of the system is characterised by a set of modes. The aim is to design a binary controller which achieves the state regulation. The switching conditions of the control law are determined by a Lyapunov function. In this approach, adjacency constraints are considered in the hybrid model to improve the performances of the converter. An experimental comparative study with the classical pulse-width-modulation strategy highlights the efficiency and the robustness of the proposed approach.**

Index Terms— **Multicellular converter, Binary controller, Dynamic hybrid system.**

I. INTRODUCTION

The power electronic concepts find an important place in the transport field. Trains, airplane, hybrid cars constitute an interesting domain for the development and optimization of electrical systems. Since the 1950s, power converters are installed in the traction system, power supplies or numerical amplifiers. A power converter ensures an adaptation of the electrical energy between a source and a load. The research in automatic control is interested in this technology because it is a major element to control the electrical energy and the regulation of motorised systems [1], [2]. For instance, converters are used to regulate the speed of a train or the position in the robotic field. Their disadvantages are due to their structures. These systems are composed of semiconductor components (transistor, IGBT, MOSFET, diode) which switch [3]. The generated waveform has harmonic contents which may accelerate the damages of the load and semiconductors.

This paper is interested in the control of the multicellular converter. It is composed of an assembly of commutation cells and secondary sources, realized by floating capacitors [4], [5]. Its structure imposes a simultaneous regulation of the internals voltages of the converter and the output current to ensure the tracking of a reference trajectory [6], [7], [8], [9]. In comparison with the classical H-bridge, an appropriate control allows to reduce the harmonic contents of the waveform and the losses due to the commutations of power semiconductors [10], [11]. Therefore, the multicellular converter offers more capacities than a classical H-bridge.

Univ. Lille Nord de France, F-59000 Lille, France; CNRS, FRE 3304, F-59313 Valenciennes, France; UVHC, LAMIH, F-59313 Valenciennes, France Jeremy.VanGorp@univ-valenciennes.fr, Michael.Defoort@univ-valenciennes.fr, Mohamed.Djemai@univ-valenciennes.fr

The classical control of this converter is first realized through the continuous variables. A PWM (pulse-width-modulation) strategy is then applied to adapt the control in the converter. In this case, the control signal is sampled [12] and the global system follows a non-linear average model [13], [14]. The objective is to reduce the error between a desired continuous signal and an average signal resulting from the model. Others controllers are proposed in the literature, for example the linearised non-linear model [15], a passivity based control [16] and a stabilizing method using Lyapunov functions [17].

It could be interesting to control the converter using an exact and instantaneous model. Here, the multicellular converter is considered as a hybrid dynamic system. Therefore, the used model takes into account the behaviours of the discrete and continuous variables [18], [19]. That is why, the dynamics of the system is defined by a set of modes. On the same idea developed by Defay et al. in [14], the harmonic contents can be reduced when the variation of the output voltage is limited by the adjacency constraints on the hybrid model. The idea is to define a binary control using a Lyapunov function satisfying these constraints. Hence, our objective is to present a robust strategy where the control variables directly represent the discrete state of the converter such that the performances are improved.

The paper is organized as follows. In Section II, the multicellular converter model is introduced. In Section III, a binary strategy is designed to control the converter associated to an inductive load. The adjacency constraints of the hybrid model are presented in Section IV. Section V highlights the efficiency of the control by a experimental comparison between a classical PWM control and the binary control.

II. MULTICELLULAR CONVERTER MODELLING ASSOCIATED TO AN INDUCTIVE LOAD

The first objective of a power converter is to transfer the energy from a primary source to a load. A second one is to adapt the control of the converter to minimize the energetic losses. The multicellular converter is based on an assembly of elementary cells of commutation. This association allows to obtain more degrees of freedom for the control.

A hybrid modelling allows to take into account the behaviours of the discrete and continuous variables. A discrete variable is addressed for each commutation cell. Therefore, a hybrid control can choose the discrete state needed to ensure

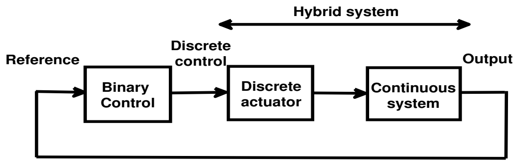

Fig. 1. Hybrid control synoptic.

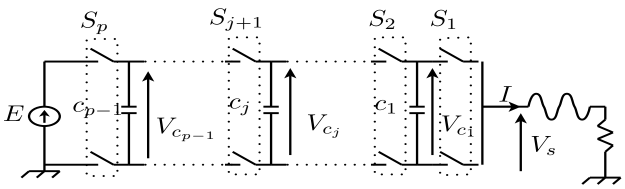

Fig. 2. Multicellular converter associated to an inductive load.

the regulation of the continuous state of the converter. Fig. 1 presents the synoptic of the hybrid control.

Fig. 2 depicts the topology of a converter with p independent commutation cells associated to an inductive load. The independency is due to the $(p-1)$ internal capacitors and can be considered only for a few switching periods. As a matter of fact, the current flows from the source E to the output I through different converter switches. This structure of the converter can't supply a negative load current, other topologies of this converter exist to create an alternative current [20]. The multicellular converter shows, by its structure, a hybrid behavior due to discrete variables (i.e. switching or commutation logic). One can refer to [21] for details. Note that because of the presence of capacitors, there are also continuous variables (i.e. currents and voltages).

It is important to highlight that in order to standardize the industrial production, the electrical switches constraints should be similar. This requirement implies a unique voltage constraint of $\frac{E}{p}$. Thus, it is necessary to ensure an equilibrated distribution of the capacitor voltages. Under these conditions, the reference voltage of the capacitor j $(j = \{1, \ldots, p-1\})$ is given by:

$$V_{c_j,ref} = j\frac{E}{p} \tag{1}$$

The dynamics of the converter, with a load consisting in a resistance R and an inductance L, is given by the following differential equations:

$$\left\{ \begin{array}{lcl} \dot{I} & = & -\frac{R}{L}I + \frac{E}{L}S_p - \sum_{j=1}^{p-1} \frac{V_{c_j}}{L}(S_{j+1} - S_j) \\ \dot{V}_{c_j} & = & \frac{I}{c_j}(S_{j+1} - S_j), \quad j = 1, \ldots, p-1 \end{array} \right. \tag{2}$$

where I is the load current, c_j is the capacitance, V_{c_j} is the voltage in the $j-$th capacitor and E is the voltage of the source.

1

Each commutation cell is controlled by the binary input signal $S_j \in \{0, 1\}$. Signal $S_j = 1$ means that the upper switch of the $j-$th cell is "on" and the lower switch is "off" whereas $S_j = 0$ means that the upper switch is "off" and the lower switch is "on".

The principle of the proposed controller is to determine the evolution of the control signals S_j such that the multicellular converter supplies the load current I as close as possible to the desired load current I_{ref} and simultaneously ensures the stability of the voltages across each cell.

III. Binary signals design

In this Section, the objective is to design a direct control law for the multicellular converter. We will see that acting directly on the control signals allows to ensure the regulation of the floating voltages and the output current.

The control algorithm is based on the redundancy of the state of the converter in order to obtain the different voltage levels at the converter output and at the terminals of the floating capacitors. This algorithm enables to directly and independently use the different voltage levels.

Let us consider the following candidate Lyapunov function:

$$V = \frac{L(I - I_{ref})^2}{2} + \sum_{j=1}^{p-1} \frac{c_j(V_{c_j} - V_{c_j,ref})^2}{2} \tag{3}$$

Since there is no jump, V is positive, continuous and null only for $I = I_{ref}$ and $V_{c_j} = V_{c_j,ref}$, $j = 1, \ldots, p-1$. Using (2), its time derivative, which depends on the value of the control signals, is as follows:

$$\begin{array}{rcl} \dot{V} & = & (I - I_{ref})\left(-L\dot{I}_{ref} - RI + ES_p\right) \\ & & -(I - I_{ref})\left(\sum_{j=1}^{p-1} V_{c_j}(S_{j+1} - S_j)\right) \\ & & +\sum_{j=1}^{p-1}(V_{c_j} - V_{c_j,ref})I(S_{j+1} - S_j) \end{array} \tag{4}$$

Let us denote

$$A_j = -(I - I_{ref})V_{c_j} + (V_{c_j} - V_{c_j,ref})I \tag{5}$$

Expression (4) can be rewritten as:

$$\begin{array}{rcl} \dot{V} & = & (I - I_{ref})\left(-L\dot{I}_{ref} - RI + ES_p\right) \\ & & -\sum_{j=1}^{p-1} A_j(S_j - S_{j+1}) \end{array} \tag{6}$$

Under the control law:

$$S_p = \frac{1 - \mathrm{sign}\,(I - I_{ref})}{2} \tag{7}$$

$$S_j = \frac{1 + \mathrm{sign}\,(A_j)}{2} \quad \forall j = 1, \ldots, p-1 \tag{8}$$

the multicellular converter supplies the load current I as close as possible to desired load current I_{ref} while ensuring a suitable distribution of the voltages across each cell. Therefore, the signum functions of (7) and (8) directly define the discrete state of the system. The signum function is described as:

$$\mathrm{sign}\,(x) = \left\{ \begin{array}{lll} 1 & \text{if} & x \geq 0 \\ -1 & \text{if} & x < 0 \end{array} \right. \tag{9}$$

Indeed, from (8), one can notice that:

$$\begin{array}{lll} \text{if } A_j \geq 0 & \text{then} & S_j = 1 \\ \text{if } A_j < 0 & \text{then} & S_j = 0 \end{array} \tag{10}$$

Therefore, since $S_{j+1} = 0$ or $S_{j+1} = 1$, the term $A_j(S_j - S_{j+1})$ of (6), is positive or null.

Due to electrical reasons, the load current is considered such that $E \geq RI \geq 0$ with $I \geq 0$. Assuming that $L\dot{I}_{ref}$ is enough small, the quantities $(-L\dot{I}_{ref} - RI + E)$ and $(RI + L\dot{I}_{ref})$ are positive. Furthermore, from (7), one can easily notice that:

$$\begin{array}{lll} \text{if } I - I_{ref} \geq 0 & \text{then} & S_p = 0 \\ \text{if } I - I_{ref} < 0 & \text{then} & S_p = 1 \end{array} \tag{11}$$

Hence, the term $(I - I_{ref})\left(-L\dot{I}_{ref} - RI + ES_p\right)$ of (6), is negative or null.

Hence, one can conclude that $\dot{V} \leq 0$. The asymptotic stability is therefore guaranteed using the proposed binary control.

IV. Hybrid strategy for adjacency constraint requirements

Let us consider the multicellular converter which is composed of p cells. Each commutation cell j is controlled by the binary signal S_j. Therefore, the hybrid control strategy is defined by 2^p modes. The proposed control of the previous section creates a stairs behaviour of the output voltage. In order to reduce the harmonic contents and the switching losses of semiconductors during the different commutation, the control limits the variation of the output voltage of E/p. Indeed the control operates one cell at once. This condition implies that the number of links between the different modes are limited to $2p$.

The marking of one mode is represented by:

$$M = [M_1 \dots M_q \dots M_{2^p}]^T \tag{12}$$

where $M_q \in \{0, 1\}$, $q = 1, \dots, 2^p$ and $\sum_{i=1}^{2^p} M_q = 1$. If the q^{th} mode is activated then $M_q = 1$. Reciprocally, if this mode is inactivated then $M_q = 0$. From the binary control of the converter $S_j \in \{0, 1\}$, the active mode q is determined by the following relationship:

$$q = 1 + \sum_{j=0}^{p-1} 2^j S_{j+1} \tag{13}$$

Under the binary controller described in the previous section, (13) leads to the marking M_d of the desired mode which enables to fulfil the control objective.

At each sampling time, the control system may choose between $p + 1$ actions in order to satisfy the adjacency constraint. Indeed, from the q^{th} mode, the system can stay in this mode or change among p other modes. Let us define the adjacency matrix $C_a \in \{0, 1\}^{2^p \times 2^p}$ which indicates the presence of transitions from one mode to another one. From the adjacency matrix, one can deduce if the system can commute from mode M toward mode M_d, i.e.

$$\mathcal{O} = M_d C_a M \tag{14}$$

where M represents the marking of the actual mode of the system and M_d the actual marking of the desired mode.

TABLE I

The different modes associated to a 3-cells converter.

Mode	1	2	3	4	5	6	7	8
$S1$	0	1	0	1	0	1	0	1
$S2$	0	0	1	1	0	0	1	1
$S3$	0	0	0	0	1	1	1	1

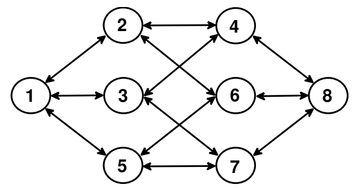

Fig. 3. Hybrid automata for a 3-cells converter.

If $\mathcal{O} = 1$, then the proposed binary controller is directly applied since the adjacency constraint is verified. Otherwise, the following strategy is applied to avoid deadlock.

When there is a deadlock, i.e. $\mathcal{O} = 0$, the system switches toward a mode which satisfy the adjacency constraint while minimizing the tracking errors. That is why, this mode is chosen to minimize the time derivative of the Lyapunov function V. The hybrid control strategy can be summarized as follows:

$$M_{applied} = \begin{cases} M_d & \text{if } \mathcal{O} = 1 \\ M_{opt} & \text{if } \mathcal{O} = 0 \end{cases} \tag{15}$$

where M_{opt} is the marking of the optimal mode such that $\dot{V}$ is minimized while satisfying the adjacency constraint.

Remark 1: When the converter is composed of more legs (i.e. for instance with a DC motor), each leg is considered as an independent hybrid system. Therefore, the adjacency constraints associated to each leg are defined by the same strategy. Furthermore, the initial conditions of each leg are not necessary similar.

Example 1: Let us consider the converter with $p = 3$ cells. (13) yields Table I. Fig. 3 depicts the 3-cells converter in the form of a hybrid automata. One can notice the adjacency constraint. Indeed, from one mode, there are only four outgoing transitions.

The links from the q'^{th} mode toward the q^{th} mode characterize the adjacency matrix C_a given in Table II. Without loss of generality, we assume that the actual mode is 1, i.e. $M = [1, 0, 0, 0, 0, 0, 0, 0]^T$. Then, we compute the binary control law as discussed in the previous section.

If it leads, for instance, to the desired mode 2, i.e. $M_d = [0, 1, 0, 0, 0, 0, 0, 0]^T$, then $\mathcal{O} = 1$. Hence, the binary control law can be directly applied.

If it leads, for instance, to the desired mode 8, i.e. $M_d = [0, 0, 0, 0, 0, 0, 0, 1]^T$, then $\mathcal{O} = 0$. Hence, we choose the optimal mode between modes 1, 2, 3 and 5, the one which minimizes $\dot{V}$.

TABLE II

ADJACENCY MATRIX C_a FOR A 3-CELLS CONVERTER.

$q' \rightarrow q$	1	2	3	4	5	6	7	8
1	1	1	1	0	1	0	0	0
2	1	1	0	1	0	1	0	0
3	1	0	1	1	0	0	1	0
4	0	1	1	1	0	0	0	1
5	1	0	0	0	1	1	1	0
6	0	1	0	0	1	1	0	1
7	0	0	1	0	1	0	1	1
8	0	0	0	1	0	1	1	1

Remark 2: In order to minimize the number of commutations, it is convenient to add a further step. Indeed, in the case that $\mathcal{O} = 0$, we can first compute the following marking:

$$M_{com} = diag(C_a M) C_a M_d \qquad (16)$$

It indicates the common adjacent modes of M and M_d. In this case, if there are common adjacent modes, we choose between them the one which minimizes $\dot{V}$.

Example 2: Let us consider the previous example. We assume that the actual mode is 1, i.e. $M = [1,0,0,0,0,0,0,0]^T$. Then, we compute the binary control law as discussed in the previous section. If it leads, for instance, to the desired mode 4, i.e. $M_d = [0,0,0,1,0,0,0,0]^T$, then $\mathcal{O} = 0$. Then, (16) leads to $M_{com} = [0,1,1,0,0,0,0,0]^T$. Hence, we choose the optimal mode between modes 2 and 3, the one which minimizes $\dot{V}$.

V. EXPERIMENTAL RESULTS

To illustrate the efficiency of the proposed control, experimental results are carried out with a three cells converter connected to a RL load. The state of the converter is determined by three control signals S_1, S_2 and S_3. The system is modelled by (2) with $p = 3$.

A. Experimental setup

To demonstrate the effectiveness of the proposed strategy, experimental investigations have been realized on a test bench which consists of a three cells converter. The schematic view of the overall platform is shown in Fig. 4. The experimental setup [6], (see Fig. 5) is described as follows.

- The power block is composed of a 3 cells converter with three legs. It is used for pedagogic or research applications. The nominal bench characteristics, obtained after identification, are:

$$c_1 = 40.10^{-6}(F), \;\; c_2 = 40.10^{-6}(F).$$

  The voltage of the source is $E = 30(V)$. Therefore the reference of the floating voltage of capacitors V_{c_1} and V_{c_2} are defined by:

$$V_{c_1,ref} = 10(V) \quad and \quad V_{c_2,ref} = 20(V)$$

- The measurement part is composed of voltage sensors to measure the voltage across the floating capacitors and a current transductor to measure the load current. A low pass filter has been added.

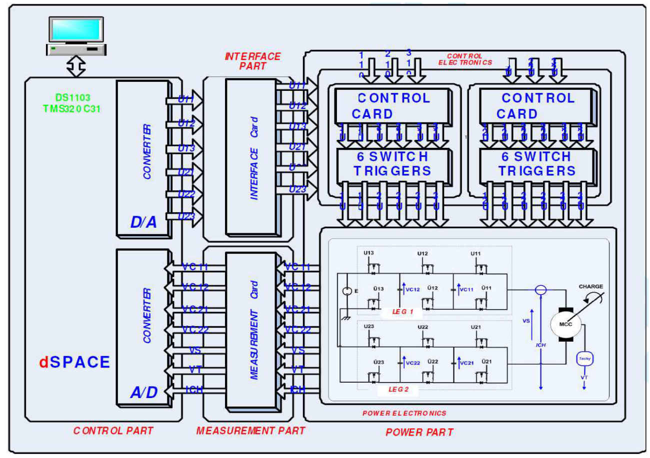

Fig. 4. Schematic view of the overall platform.

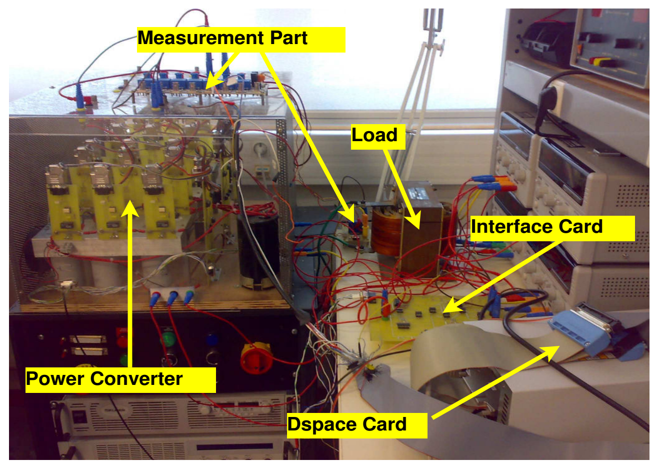

Fig. 5. Photography of the experimental setup.

- The computer is equipped with Mathworks softwares and an interface dSPACE card DSP1103, based on a floating point DSP (TMS320C31) of frequency $50(MHz)$ with ControlDesk software in order to visualize the state during the experiment. In order to have the best resolution, the minimum sampling period for the Dspace has been chosen, i.e. $T_{ech} = 10^{-4}(s)$.
- The three control inputs, designed by the proposed scheme, are computed and delivered by the interface dSPACE card. An interface card allows to protect, by insulation, the DSP of the power electronics.
- The load is composed of an inductance and a resistance:

$$R = 6(\Omega), \;\; L = 0.0006(H).$$

In order to analyse the performances of the controller, we compare the experimental results between a classical PWM strategy and the proposed binary controller. One should highlight that no filter is used. For a fair comparison between classical PWM and the proposed binary control, the sampling

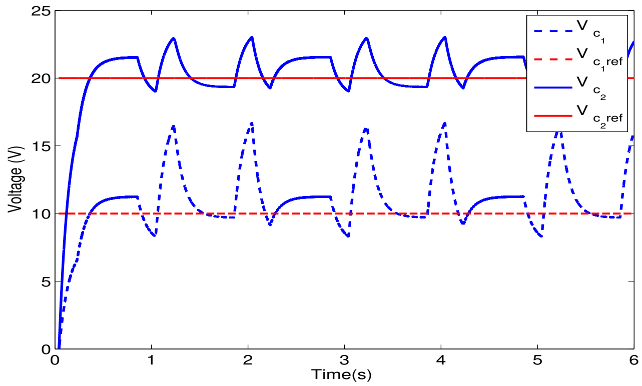

Fig. 6. Evolutions of voltages V_{c_1} and V_{c_2} using the PWM strategy.

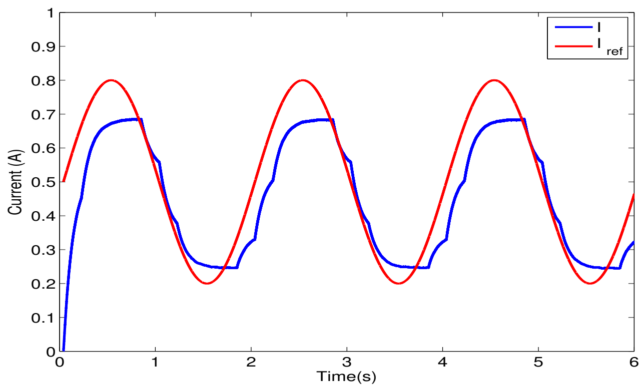

Fig. 7. Evolution of load current I and its reference I_{ref} using the PWM strategy.

period is $10^{-4}(s)$ for both experimentation.

B. Classical PWM

The strategy of this control is based on the average model. A duty cycle variation allows to stabilize the load current and the voltages of the floating capacitors around the desired values. The three control signals are determined by the comparison of the reference current I_{ref} and three triangular signals of period T and dephasing of $T/3$ (see [20], [6]). Fig. 6 shows the waveforms of the voltages across the floating capacitors and Fig. 7 depicts the load current for $T = 0.001(s)$.

It can be noted that the current has a tracking error and the capacitor's voltages are stabilized around the desired values. Nevertheless, this control produces important oscillations on the state.

C. Binary Control

Figs. 8 and 9 show respectively the waveforms of the voltages V_{c_1}, V_{c_2} and the load current I. One can see that the control fulfills the desired objective. different figures highlight the robustness of the proposed binary controller. One can see that the state of the system, defined by (2), follows the reference trajectory.

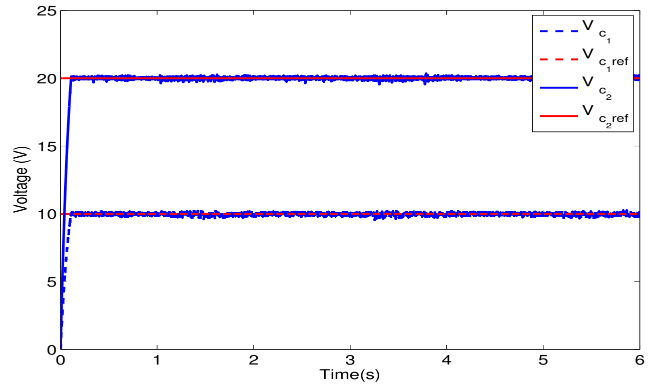

Fig. 8. Evolutions of voltages V_{c_1} and V_{c_2} using the proposed binary control.

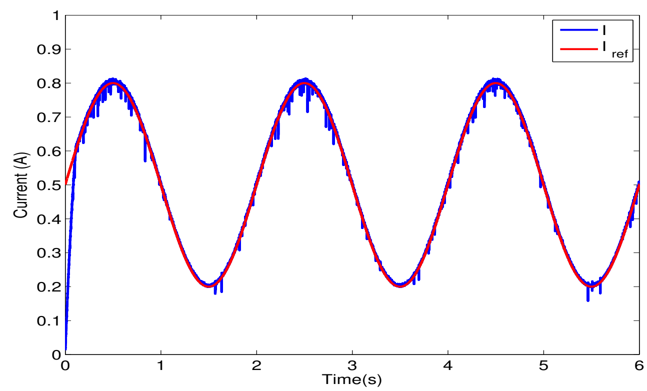

Fig. 9. Evolution of load current I and its reference I_{ref} using the proposed binary control.

Figure 10 shows the evolution (zoom) of the output voltage. One can remark that the maximum variation is $E/3 = 10(V)$, therefore the adjacency constraints are verified. Fig. 11 highlights the reduction of the harmonic contents. The spectrum (i.e. FFT of the load current) associated with the PWM control shows the harmonic contents corresponding to the sampling period $T = 0.001(s)$.

Table III summarizes the obtained experimental results for the classical PWM and the binary controller. One can see that the robustness properties, the accuracy and the convergence rate are improved using the proposed strategy compared to the PWM scheme.

The binary control of the multicellular converter associated to an other load would show a larger error. Indeed, if the load

TABLE III
COMPARISON BETWEEN THE PWM AND THE BINARY CONTROL LAW.

	PWM	Binary control
Duration of the transient	$0.25(s)$	$0.11(s)$
Error max on V_{c_1}	$6.66(V)$	$0.4(V)$
Error max on V_{c_2}	$3.05(V)$	$0.3(V)$
Error max on I	$0.17(A)$	$0.04(A)$

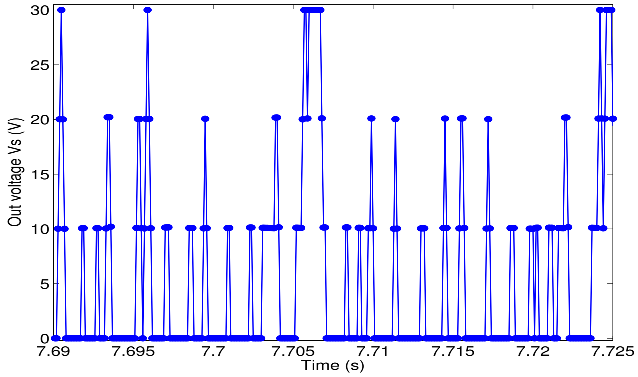

Fig. 10. Output voltage V_s using the proposed binary control (ZOOM).

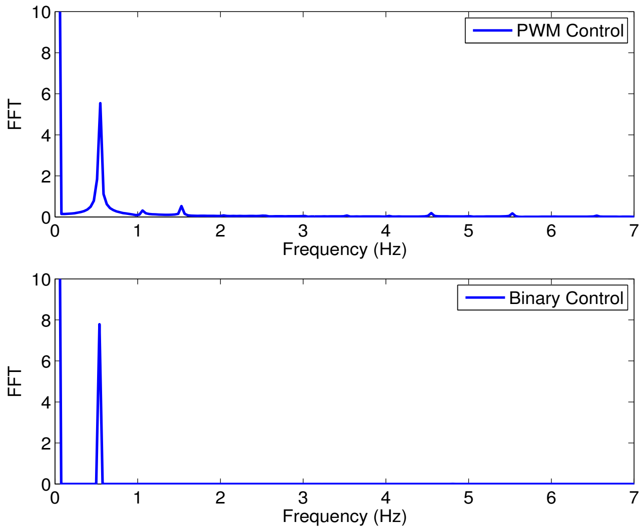

Fig. 11. Spectrum comparison for both control strategies (i.e. FFT of the load current).

is composed of a lower inductance and a bigger resistance then the output current should be less filtered.

VI. Conclusion

In this paper, a control law for the multicellular converter is designed in order to ensure both load current tracking and capacitors voltages balancing. A controller based on the hybrid formalism and Lyapunov function is proposed. The adjacency constraints are also defined to reduce the harmonic contents and to improve the performances of the converter. An experimental comparative study with the classical pulse-width-modulation strategy has shown the efficiency and the robustness of the proposed approach. Further works aim at estimating the internal voltages of the capacitors using an observer.

VII. Acknowledgement

This work has been supported by International Campus on Safety and Intermodality in Transportation, the European Community, the Delegation Regionale a la Recherche et a la Technologie, the Ministere de l'Enseignement suprieur et de la Recherche, the Region Nord Pas de Calais, the Centre National de la Recherche Scientifique and GIS-3SGS under the project DICOP, $n°3SGS - 11 - 03 - 01$.

References

[1] Fakham H., Djemaï M. and Busawon K., "Design and practical implementation of a back EMF sliding mode observer for a brushless DC motor", *IET Electric Power Applications*, **2**(6), pp. 353–361, 2008.
[2] Escalante M.F., Vannier J.-C. and Arzande A., "Flying capacitor multilevel inverters and dc motor drive applications", *IEEE Trans. on Ind. Electronics*, **49**(4), pp. 809–815, 2002.
[3] Erickson R. and Maksimovic D., "Fundamentals of Power Electronics", *Second Edition, Kluwer Academic Publishers, Dordrecht*, The Netherlands, 2001.
[4] Meynard T. and Foch H., French patent N91,09582 du 25 juillet 1991, dpt international PCT (Europe, Japon, USA, Canada), N92,00652 du 8 juillet 1992, 1991.
[5] Meynard T., Foch H., Thomas P., Courault J., Jakob R. and Nahrstaedt M., "Multi-cell converters: basic concepts and industry applications", *IEEE Trans. on Ind. Applications*, **49**(5), pp. 955–964, 2002.
[6] Djemaï M., Busawon K., Benmansour K. and Marouf A., "High order sliding mode control of a DC motor via a switched controlled multi cellular converter", *Int. J. of Systems Science*, 2011 (to appear).
[7] Defoort M., Djemaï M. and Floquet T. and Perruquetti W., "Robust finite time observer design for multicellular converters", *Int. J. of Systems Science*, 2011 (to appear).
[8] Defoort M., Nollet F., Floquet T. and Perruquetti W., "A third order sliding mode controller for a stepper motor", *IEEE Trans. on Ind. Electronics*, **56**(9), pp. 3337–3346, 2009.
[9] Utkin, V. "Sliding Mode Control Design Principles and Applications to Electric Drives", *IEEE Trans. on Ind. Electronics*, **40**(1), pp. 23–36, 1993.
[10] Beaudesson P., "Sûreté de fonctionnement, reconfiguration et marches dégradées des convertisseurs multiniveaux IGBT", PhD Thesis, INP Toulouse, 2000.
[11] Bethoux O., and Barbot J.P., "Multi-cell chopper direct control law preserving optimal limit cycles", *Proc. of CCA* Glasgow, **2**, pp. 1258–1263, 2002.
[12] Bhagwat P.M. and Stefanovic V.R., "Generalized structure of a multi-level PWM inverter", *IEEE Trans. on Ind. Applications*, **32**, pp. 509–517, 1996.
[13] Sira-Ramirez H., "Non linear p-i controller design for switch-mode dc-to-dc power converters", *IEEE Trans. on circuits and systems*, **38**, pp. 410–417, 1991.
[14] Defay F., Llor A.-M., Fadel M., "A Predictive Control With Flying Capacitor Balancing of a Multicell Active Power Filter", *IEEE Trans. on Ind. Electronics*, **55**(9), pp. 3212–3220, 2008.
[15] Gateau G., Fadel M., Maussion P., Bensaid R. and Meynard T., "Multicell converters: active control and observation of flying capacitor voltages", *IEEE Trans. on Ind. Electronics*, **49**(5), pp. 998–1008, 2002.
[16] Sira-Ramirez H., Moreno R.P., Ortega R., Esteban, M.G., "Passivity-based controllers for the stabilization of dc-t-dc power converters", *Automatica*, **33**, pp. 499–513, 1997.
[17] Baja M., Patino D., Cormerais H., Riedinger P. and Buisson J., "Hybrid control of a three-level three-cell dc-dc converter", *American control conference*, pp. 5458–5463, 2007.
[18] Benmansour K., Tlemani A., Djemaï M., and De Leon J., "A New Interconnected Observer Design in Power Converter: Theory and Experimentation", *Nonlinear Dynamics and Systems Theory*, **10**(3), pp.211–224, 2010.
[19] Meynard T., Fadel M. and Aouda N., "Modeling of multilevel converters", *IEEE Trans. on Ind. Electronics*, **44**(3), pp. 356–364, 1997.
[20] Benmansour K., "Ralisation d'un banc d'essai pour la Commande et l'Observation des Convertisseurs Multicellulaires Srie : Approche Hybride", PHD Thesis, Universit de Cergy, Juin 2009.
[21] Barbot J.P., Saadaoui H., Djemaï M. and Manamanni N., "Nonlinear observer for autonomous switching systems with jumps", *Nonlinear Analysis: Hybrid Systems*, pp. 537–547, 2007.